Journal of the Optical Society of Korea, Vol. 10, No. 1, March 2006, pp. 42-47

Murine Heart Wall Imaging with Optical Coherence Tomography

Jee-Hyun Kim*

Beckman Laser Institute and Medical Clinic, University of California at Irvine, Irvine, CA, 92612 USA

Byeong Ha Lee

Department of Information and Communications, Gwangju Institute of Science and Technology, Oryong-dong, Buk-gu, Gwangju 500-712, KOREA

(Received February 7, 2006 : revised February 7, 2006)

M-mode imaging of the *in vivo* murine myocardium using optical coherence tomography (OCT) is described. Application of conventional techniques (e.g. MRI, Ultrasound imaging) for imaging the murine myocardium is problematic because the wall thickness is less than 1.5 mm (20 g mouse), and the heart rate can be as high as six hundred beats per minute. To acquire a real-time image of the murine myocardium, OCT can provide sufficient spatial resolution (10 μm) and imaging speed (1000 A-scans/s). Strong light scattering by blood in the heart causes significant light attenuation, which makes delineation of the endocardium-chamber boundary problematic. To measure the thickness change of the myocardium during one heart beat cycle, a myocardium edge detection algorithm is developed and demonstrated.

OCIS codes : 110.4500, 170.0170, 120.3890

I. INTRODUCTION

Use of a murine model for cardiovascular research has many advantages. First, murine heart function is similar to that in humans. Second, modest resource requirements make the model attractive. Third, maturation is readily attained over a short period of time. Finally, because the murine genome is well characterized and can be easily modified, cardiovascular molecular mechanisms can be investigated through gene alterations.

A reliable imaging technique to determine regional wall thickening in intact beating mouse hearts has not been realized even though monitoring the myocardium thickness is an important factor of cardiovascular diagnostics. Conventional methods, such as ultrasound and MRI, are either too slow to show the beating heart or too expensive for everyday lab use, and do not provide sufficient spatial resolution for the small dimensions of the murine heart. Optical coherence tomography (OCT), as a promising new technique, may be an appropriate imaging modality for murine cardiovascular studies. OCT is analogous to ultrasound, measuring the intensity of backscattered light rather than sound waves. Since light travels faster than sound and has a substantially shorter wavelength, the use of OCT can provide micron scale resolution [1] and faster-than-video imaging speeds [2]. Moreover, the relative simplicity of the instrumentation allows for inexpensive construction.

Early biomedical applications of OCT focused on imaging stationary and transparent tissues such as eyes, where imaging depths could be deeper than 2 cm [3,4]. Further developments have focused on non-transparent, highly scattering tissues, such as skin, where structures as deep as 1-2 mm have been visualized [5]. Dynamic, but nearly transparent, structures such as the developing *in vivo* tadpole heart, have also been studied using OCT [6]. Although Doppler OCT has been used to assess *in vivo* blood flow, the problem of blood attenuation was noted [7].

Recently, there has been increasing interest in applying OCT to the cardiovascular system. Intravascular imaging has been achieved *in vivo* with a rabbit aorta [8]. In vitro studies with coronary arteries suggest a method of determining fibrous cap thickness of atherosclerotic plaques [9,10]. Despite these recent successes, cardiovascular imaging with OCT remains problematic primarily due to the strong attenuation of light by blood. Light attenuation in blood originates from two sources - absorption by hemoglobin and scattering by

red blood cells [11-13]. Kramer et al [14] showed that light attenuation in whole blood is 7-20 times stronger than that in a solution with the same concentration of hemoglobin. The attenuation of light in whole blood is mainly due to scattering, therefore, in general, it is difficult to acquire a relatively clear image of the sample submerged in blood. A degraded image can be recovered by use of a proper image processing technique. We have tried several edge detection algorithms such as Sobel, Robert, Prewitt, Zero-cross, Canny, and Median filters. However, a single application of each filter could not clearly detect any wall boundary.

In this study, we want to investigate whether OCT can be applied to a dynamic and non-transparent biological structure such as the murine right ventricle that has a thin anterior chamber. Physiological observation on the movement of the heart muscle could reveal that there is strong coupling between the outer and inner boundaries. However, as mentioned, due to the high scattering from blood in the heart chamber, the OCT image is blurry. Therefore, we propose an edge enhancement algorithm that can clearly distinguish the heart wall boundaries from a blurry OCT image of a murine heart. The proposed algorithm combines several nonlinear filters, such as 2D median filter, open/close filter, and using threshold and polynomial tracing methods. Polynomial fitting of the well-defined outer boundary of the heart is found at first, and then, with this information the inner boundary is estimated.

II. EXPERIMENTAL SETUP

2.1 *System Description*

OCT is an interferometric technique based on a white-light interferometer. The principles of OCT have been widely reported [1]. Our OCT system as shown with Fig. 1 was based on a single-mode optical fiber Michelson interferometer. Where, we have used a semiconductor optical amplifier (SOA) as the broadband light source and a rapid scan optical delay (RSOD) line [2] as the scanning arm. The SOA had a center emission wavelength of 1310 nm and a spectral bandwidth of 60 nm. To visualize the light incident on a murine myocardium for unaided eyes, 630 nm red light was co-launched to the fiber with a wavelength division multiplexer (WDM). Position of the incident light was perpendicularly fixed on the epicardium without any lateral scanning. The optical power incident on the target was 3.65 mW. The RSOD enabled us to acquire 400 A-scans per second, which was suitable for imaging a dynamic tissue like a beating murine heart at a video rate. The axial and lateral resolutions were 16 μm and 12 μm, respectively. One A-scan (a depth scan) corresponded to 2 mm in air and comprised 5000 two-byte data samples, corresponding to a time of 2.5 ms at a

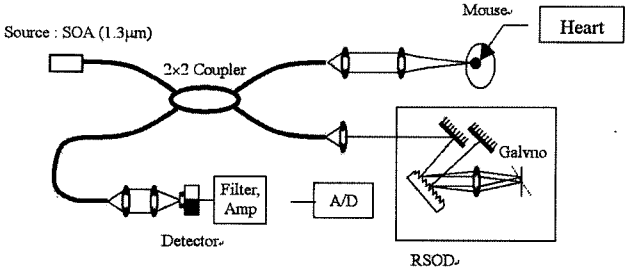

FIG. 1. OCT system diagram for murine myocardial imaging. SOA: Semiconductor optical amplifier; A/D: analog to digital converter; RSOD: Rapid Scanning Delay Line.

2 MS/s sampling rate. One M-mode scan consisted 400 A-scans per second. To achieve real time data acquisition and signal processing, the Labview software (National Instruments, Austin, TX) was used. After detection with a photodiode, a band-pass filter was used to remove unwanted low and high frequency noise, and an incoherent demodulation method was used to compensate for non-linearities in the galvanometer scanning.

2.2 *Animal Protocol*

The protocol was approved by the Institutional Animal Care and Use Committee at The University of Texas at Austin and San Antonio, and conformed with "Guidelines for the Care and Use of Laboratory Animals" (NIH publication No. 86-23, revised in 1985) and "Principles of Laboratory Animal Care" (published by the National Society for Medical Research). Female C57-B6 mice (n = 6) weighing 19 to 22 g were anesthetized by administering urethane (1000 mg/kg, i.p.) and etomidate (25 mg/kg, i.p.). Respiration was controlled through a tracheotomy cannula and the animals were mechanically ventilated with 100% O_2 at 95 breaths per minute using a rodent ventilator (Harvard Apparatus Model 683, South Natck, MA). Needle electrodes were applied subcutaneously and connected to a Microelectrode AC amplifier (Model 1800, A-M Systems, Carlsborg, WA) for ECG recording. The chest was entered by an anterior thoracotomy. An apical stab was made in the left ventricle with a 27-G needle, through which Oxyglobin was introduced into the bloodstream. A right neck cutdown was performed and right jugular vein exposed. The right jugular vein was nicked for blood removal, or compressed for hemostasis.

The OCT light source was aimed at the right ventricular mid-free wall with the red aiming beam. Baseline images were recorded at the native hematocrit. Hematocrit was determined by centrifugation followed by comparison to a calibration chart. Oxyglobin was used to replace whole blood in a 1:1 fashion, in amounts of approximately 300 μl at a time. This process was continued until a hematocrit of less than 5% was obtained.

A 5% hematocrit threshold was determined from the *in vitro* slide study (see Results) and consistent with previously documented studies [15-17]. Images were recorded as described above and processed offline.

III. MURINE HEART THICKENING DETECTION ALGORITHM

Figure 2 shows one of the A-scan images of a beating mouse heart. As can be seen in the figure, the structure signal in the A-scan image is amplitude modulated with a carrier signal having a frequency f_c. Where, the carrier frequency f_c is proportional to the scanning speed of the reference arm. Therefore, to get only the structure signal, we need to extract the envelope information from the A-scan image. A cross-sectional image (B-scan) of a sample is constructed by juxtaposing many envelope signals obtained from A-scan images. In this study, to achieve the envelope of each A-scan, the coherent demodulation method was used.

To the signal $X_A(t)$, at first, a signal having the carrier frequency f_c is multiplied and then low pass filtered, which gives the signal X in Fig. 3. At the same time another signal having a 90 degree phase shifted against to the signal for X is multiplied and low pass filtered, which gives the signal Y in the same figure. From these manipulations, the envelope and the phase of the original signal $X_A(t)$ are simply calculated as

$$\text{Envelop of } X_A(t) = \sqrt{X^2 + Y^2} \quad (1)$$

$$\text{Phase of } X_A(t) = \tan^{-1}(X/Y) \quad (2)$$

In general, the phase information of Eq. 2 is used to get the flow velocity in a Doppler OCT system. Figure 4 shows the envelope signal obtained by demodulating the A-scan image of Fig. 2 with the method of Fig. 3 and using Eq. (1). As mentioned, by juxtaposing a series of demodulated A-scan images taken while laterally scanning, a two dimensional cross-sectional image of a murine heart can be constructed. However, in this study, the lateral scanning was not done, but a series of A-scans were made at a fixed point, which gives a M-mode image. A M-mode image taken at the beating murine heart is presented in Fig. 5. The figure shows a series of A-scan images taken during 5 heart cycles. This image has been used as the input image for developing an appropriate algorithm for the murine heart thickening measurement.

In Fig. 5, the upper boundary of the heart wall was obvious but the lower boundary was not clear. Therefore, to enhance the boundary of the image, at first, we have applied several gradient-based edge detecting filters, such as Robert, Prewitt, and Sobel filters. However, the results turned out not to be adequate for OCT image enhancement because they were so sensitive to noise. Figure 6 shows one of the edge-enhanced images obtained by applying a Sobel filter. The filtered image has many broken edges and gaps; thus, getting or distinguishing the heart wall boundary from the background signal does not look like easy. The main problem in the filtering work was the spike pattern of the original input image as can be seen with the demo-

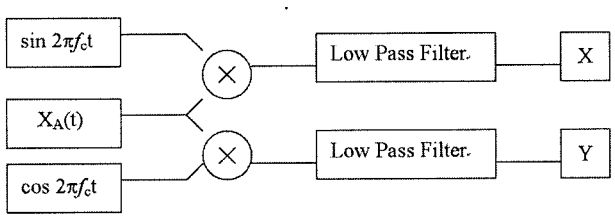

FIG. 3. Schematic diagram of coherent demodulation method.

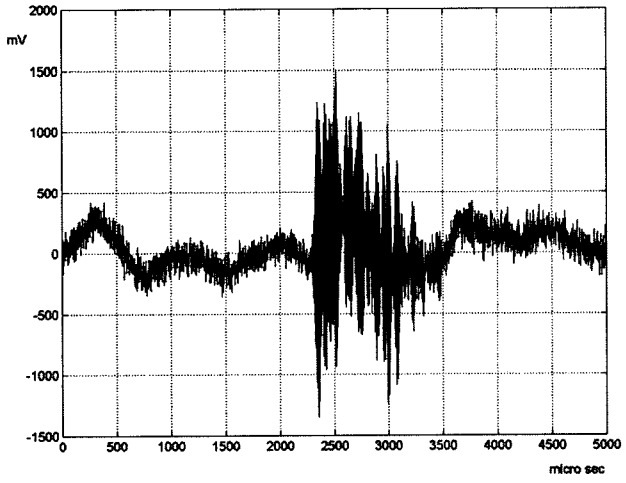

FIG. 2. A-Scan signal. It is amplitude modulated.

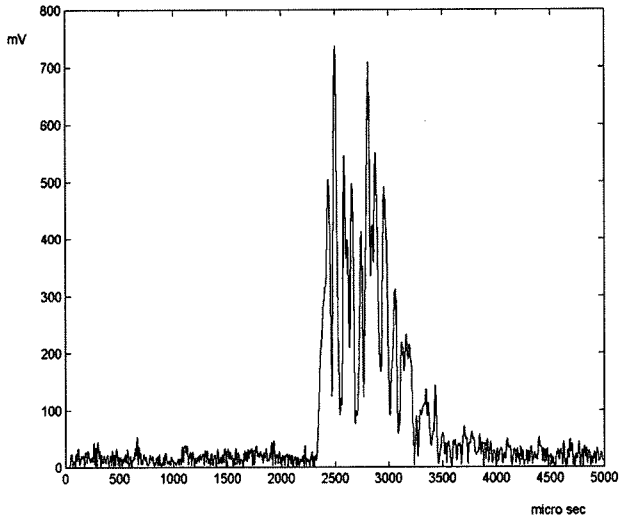

FIG. 4. Demodulated A-scan signal.

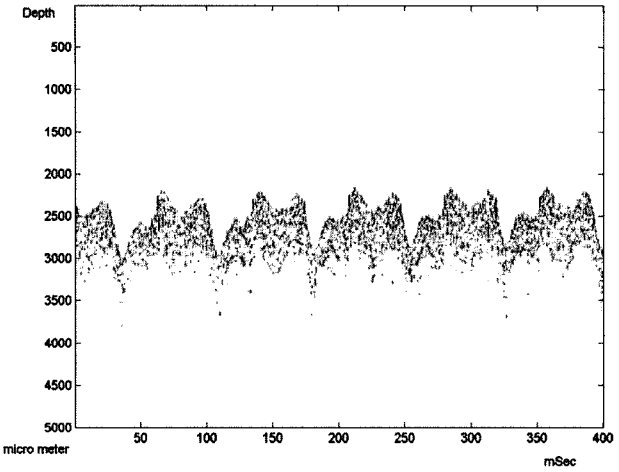

FIG. 5. M-mode image of a murine heart (correction of A-mode images taken at a point).

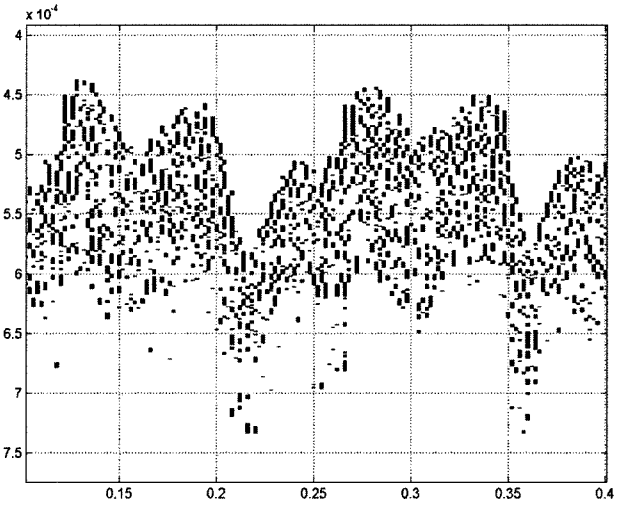

FIG. 6. Edge-enhanced image of Fig. 5. Sobel filter was used.

dulated A-scan image of Figure 4. The spike pattern works as noise. These tries evaluate that simple application of a conventional edge detecting filter is not appropriate to this kind of OCT image, so there is a need to develop a specific approach to extract the boundaries of the image.

From these necessities, we propose to combine several nonlinear filters, such as 2D median filter, open/close filter, thresholding, and polynomial tracing algorithm. The procedure of the proposed algorithm is depicted in Fig. 7. In this algorithm, an edge enhancement process was used before performing the edge detection because of the characteristics of the demodulated OCT image. At first, the gray level 2D median filtering was used to remove most spikes that worked as noise and to achieve edge preservation. Secondly, a threshold setting was used to change the gray level image into a binary level before morphological filtering. From the original

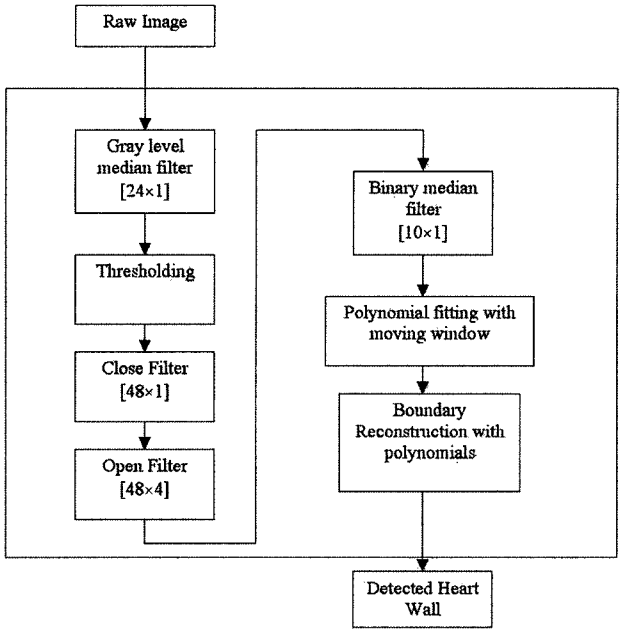

FIG. 7. Flow chart of the murine heart wall thickening detection algorithm.

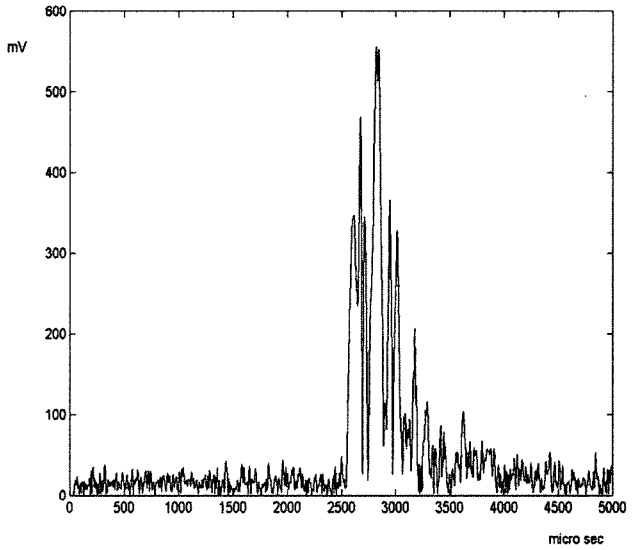

FIG. 8. Demodulated A-scan signal.

raw image of Fig. 8, by applying the 2D median filter we could get a much-simplified (less spiky) image as shown with Fig. 9.

The close and the open morphological filters were used to smooth the boundary. However, these filters could not remove most residual parts below the inner heart boundary, thus, additional binary 2D median filter were used to compensate the open and close filtering. Moreover, since the physiological heart movement could be modeled with a certain order of polynomial, the heart boundary in the image was fitted with a moving window polynomial curve. Finally, the heart wall boun-

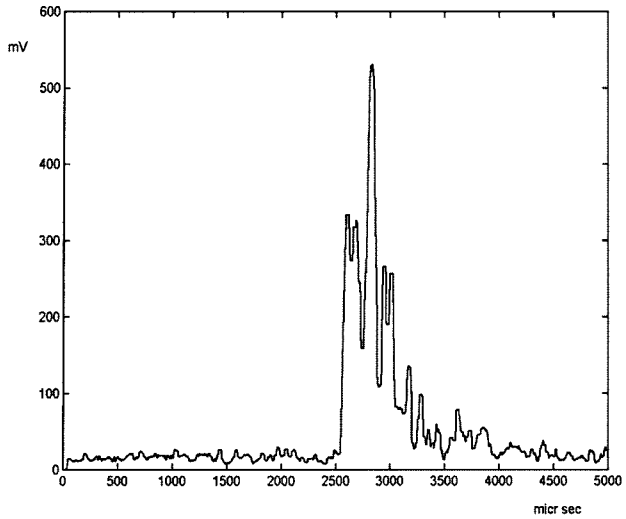

FIG. 9. Gray level median filtered A-scan signal.

dary was reconstructed. Figure 10 shows the manipulated image taken after each step of Fig. 7. The final image (Fig. 10 (g)) shows the boundary of the heart wall very clearly. We can see that the thickness varies periodically with the heart beating.

IV. DISCUSSION

The refractive index mismatch (1 : 1.4) between air and the outer heart wall was large enough to give a clear outer boundary so that there was no need of applying any edge enhancing process. However, since the inner heart wall was exposed to blood, the refractive index mismatch was small (1.4 : 1.3). Therefore, the amount of reflected light from the inner muscle was much smaller than that from the outer muscle. Because of this reason the inner boundary image was blurry.

Owing to the high refractive index mismatch at the air-muscle interface, the polynomial curve fitting to the outer boundary could be easily extracted. However, the polynomial fitting for the inner boundary was not easy even after filtering with the proposed algorithm. Therefore, the information obtained with the outer boundary was used to get the inner boundary. It is reasonable to assume that the movements of both boundaries are almost the same, except the thickness change, thus the same order of polynomial curves could be used to fit both boundaries.

A period of each heart cycle was measured by performing the Fourier transform of the epicardium boundary for the moving window size. We stored the change of the polynomial orders of the epicardium boundary as the window moved. Finally the stored corresponding polynomial order was used to fit the endocardium boundary at each moving window cycle.

V. CONCLUSION

We have presented the *in vivo* M-scan OCT image of a murine heart. The scanning rate, 400 A-scans per second, was enough to show the beating of the heart. To visualize the heart wall thickness variation during the heart beating, we have proposed a murine heart wall thickening detection algorithm mainly based on a polynomial tracing method, which turned out to be a promising edge detecting algorithm for this specific application. To overcome basic limitations of the OCT image that had different properties from traditional images, a combination of several morphological filters

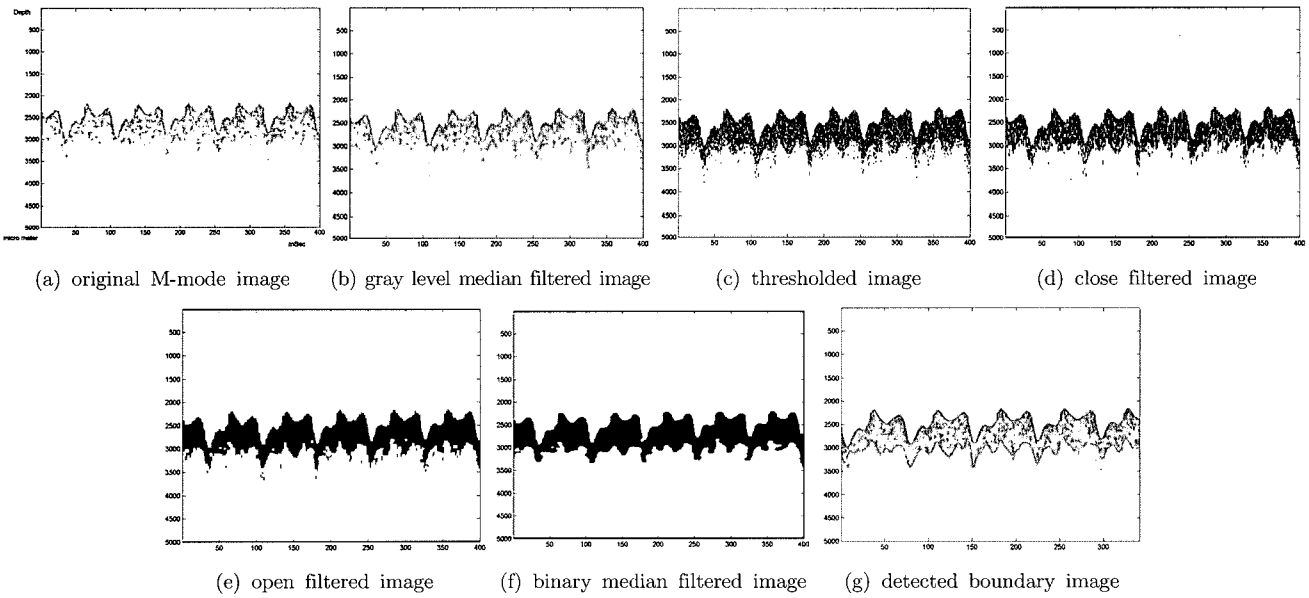

(a) original M-mode image (b) gray level median filtered image (c) thresholded image (d) close filtered image

(e) open filtered image (f) binary median filtered image (g) detected boundary image

FIG. 10. The manipulated image taken after each step.

and windowing polynomial reconstruction has been developed. We found that a gray level 2D median filter gave noise reduction (spikes) and edge preservation, open and close filters could efficiently remove unwanted spots, and additional binary 2D median filters could compensate the effect of the open and close filtered image.

The drawback of the proposed algorithm is in intensive computing power because of using many filters, so it is proper for post-processing. In this study, the threshold level was set manually, which affected the result significantly, but adaptive thresholding can improve the overall performance in future studies. The current algorithm searches only one inner boundary contour, but also it can be improved by finding several possible instances of the boundaries, finding their derivatives and comparing the most similar one with the derivatives of the outer boundary curve.

*Corresponding author : jeehk@uci.edu

REFERENCES

[1] D. Huang et al., "Optical coherence tomography," Science, vol. 254, no. 5035, pp. 1178-81, 1991.

[2] A. M. Rollins et al., "*I*n vivo video rate optical coherence tomography," Optics Express, vol. 3, no. 6, pp. 219-229, 1998.

[3] M. R. Hee et al., "Optical coherence tomography of the human retina," Archives of Ophthalmology, vol. 113, no. 3, pp. 323-332, 1995.

[4] M. G. Ducros et al., "Polarization sensitive optical coherence tomography of the rabbit eye," IEEE Journal of Selected Topics in Quantum Electronics, vol. 5, no. 4, pp. 1159-1167, 1999.

[5] J. M., Schmitt, M. J. Yadlowsky, and R. F. Bonner, "Subsurface Imaging of Living Skin with Optical Coherence Microscopy," Dermatology, vol. 191, no. 2, pp. 93-98, 1995.

[6] S. A. Boppart et al., "Noninvasive assessment of the developing Xenopus cardiovascular system using optical coherence tomography," Proceedings of the National Academy of Sciences of the United States of America, vol. 94, no. 9, pp. 4256-4261, 1997.

[7] Z. P. Chen et al., "Noninvasive imaging of in vivo blood flow velocity using optical Doppler tomography," *O*ptics Letters, vol. 22, no. 14, pp. 1119-1121, 1997.

[8] J. G. Fujimoto et al., "High resolution in vivo intra-arterial imaging with optical coherence tomography," Heart, vol. 82 no. 2, pp. 128-133, 1999.

[9] M. E. Brezinski et al., "*I*maging of coronary artery microstructure (in vitro) with optical coherence tomography," American Journal of Cardiology, vol. 77, no. 1, pp. 92-93, 1996.

[10] P. Patwari et al., "Assessment of coronary plaque with optical coherence tomography and high-frequency ultrasound," American Journal of Cardiology, vol. 85, no. 5, pp. 641-644, 2000.

[11] V. Twersky, "Absorption and Multiple Scattering by Biological Suspensions," Journal of the Optical Society of America, vol. 60, no. 8, pp. 1084-1089, 1970.

[12] A. Roggan et al., "Optical properties of circulating human blood in the wavelength range 400-2500 NM," Journal of Biomedical Optics, vol. 4, no. 1, pp. 36-46, 1999.

[13] J. M. Steinke and A. P. Shepherd, "Role of Light-Scattering in Whole-Blood Oximetry," IEEE Transactions on Biomedical Engineering, vol. 33, no. 3, pp. 294-301, 1986.

[14] K. Kramer et al., "Spectrophotometric Studies on Whole Blood in the Red and near Infrared Regions," American Journal of Physiology, vol. 159, no. 3, pp. 577-577, 1949.

[15] T. Viero and Y. N., "3-D Median structures for image sequence filtering and coding," In *Motion Analysis and Image Sequence Processing*, 1993.

[16] S. Tsekeridou, C. K., and I. Pitas, "Morphological Signal Adaptive Filter for Still Image and Image Sequence Filtering," *ISCAS '98*, no. 4, pp. 21-24, 1998.

[17] A. W. T. Lim, E. K. T., and D. P. Mital, "Edge Detection in Range Image with Multiple Window Operators," *TENCON '92*, no. 2, pp. 809-814, 1992.